

## **ADIABATIC COMPRESSED CO<sub>2</sub> ENERGY STORAGE**

**Matteo Manzoni\***

TPG-DIME, University of Genoa  
Genoa, Italy  
matteo.manzoni2012@libero.it

**Alberto Patti\***

TPG-DIME, University of Genoa  
Genoa, Italy  
albe.patti@gmail.com

**Simone Maccarini**

TPG-DIME, University of Genoa  
Genoa, Italy

**Alberto Traverso**

TPG-DIME, University of Genoa  
Genoa, Italy  
alberto.traverso@unige.it

### **ABSTRACT**

As the energy market is moving worldwide towards low-emission solutions, there is a growing interest in plants capable of storing non-dispatchable renewable power, contributing to maintain the high quality level of current electrical infrastructure and ensuring spinning-reserve capability, complementing the lack of frequency control by most of solar and wind technologies. CO<sub>2</sub> cycles, including supercritical ones, could be a solution to achieve this goal. Most of current efforts on CO<sub>2</sub> cycles are devoted to study the most promising configurations for power production, including supercritical CO<sub>2</sub> plants for solar energy conversion. Basing on such extensive state of the art and growing knowledge, this paper aims to analyse innovative energy storage solutions involving closed cycles, employing different working fluids in sub-critical or supercritical conditions, including CO<sub>2</sub>. Different plant configurations and operating conditions at 10 MWe design point are compared in terms of Round Trip Efficiency (RTE) and preliminary costs, benchmarked against traditional large scale storage solution such as CAES. Subcritical CO<sub>2</sub> cycles is shown to be a very promising solution with RTE>70% and attractive cost features, thus being a potential candidate for utility scale energy storage.

### **INTRODUCTION**

The energy demand has grown exponentially in the last 150 years due to increase in population and industrial development. According to the International Energy Agency (IEA), prior to the present sanitary

crisis, energy demand was projected to increase by 12% between 2019 and 2030. Growth over this period is now 9% in one prediction, and only 4% in another one, both made by IEA [1]. Although the recession caused by the COVID-19 pandemic, this scenario of constant increase in energy demand points out the relevance of using renewable energy sources for a sustainable future. Furthermore, in the projected change in primary energy demand by fuel in 2020 relative to 2019 by IEA, only the renewables demand is expected to increase, by 0.8%; for example, oil demand could drop by 9% [2].

Nevertheless, the main feature of renewable sources is the unpredictability, which leads to problems of adaptation to the electrical grid.

Electricity customers usually have an uneven load profile during the day, resulting in load peaks; moreover, in the last decades an increase in the general demand and the introduction of non-dispatchable renewables resulted in greater peaks of the cumulative demand curve, increasing the need of systems able to shave peaks. In fact, the power system has to be sized for that peak load while during other parts of the day it is under-utilized. The extra costs in keeping up with the peak demand are passed to the customers in form of a power fee, i.e. paying for your maximum peak load [3]. The energy storage system is controlled to be charged during off peak hours and discharged during peak hours, reducing the net peak load and hence the power fee [4]. As a result of the problems presented, the need of an intense technological development aimed at improving energy storage appears clear. Therefore, a more accurate analysis of modern energy storage systems already

operating and a research of new process that could be introduced into the future market are imperative.

Energy storage solutions available at MW scale include Battery Energy Storage System (BESS), Pumped Hydro Storage (PHS) and Compressed Air Energy Storage (CAES). Regardless, even if PHS is highly developed, efficient and effective, its main issue is the dependence on the right morphological conditions.

However, at the moment solutions are needed to overcome operational problems related to the abovementioned systems, to improve performance, storage capacity and to reduce costs.

Overall, many applications of CO<sub>2</sub> as a working fluid are studied, especially in the fields of power cycles for renewable energy (such as CSP) and waste heat recovery (WHR) [5], due to their compactness and high efficiency. Instead in this paper the CO<sub>2</sub> is seen as a possible different solution to the energy storage problem, and so appropriate configurations of CO<sub>2</sub> and S-CO<sub>2</sub> closed cycles are discussed in detail.

### ENERGY STORAGE PLANT

The plant design and the initial hypotheses regarding the thermodynamic parameters are extracted from the recent patent by Mr. Spadacini entitled “Energy Storage Plant and Process” [6], see Figure 1.

The cycle described include an energy accumulation phase (charge phase) followed by an energy release phase (discharge phase). Regarding the components, the system consists of a compressor (2), a turbine (3), a primary heat exchanger (5), a secondary heat exchanger (6), an ambient pressure tank (1), a high pressure tank (7), a motor/generator (4), a valve (8) and a non-return valve (9) as represented in Figure 1; other similar configurations are proposed in the patent but not accounted in this paper.

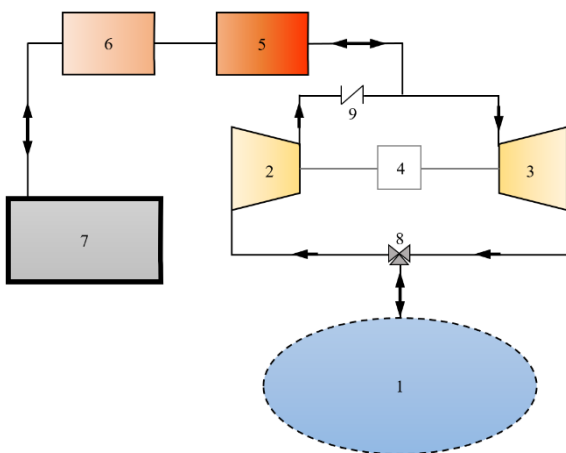


**Figure 1:** Simplified scheme of plant layout for energy storage

### SUBCRITICAL CO<sub>2</sub> STORAGE SYSTEM

In this paragraph, a CO<sub>2</sub> closed loop in subcritical regime is examined. The system includes: a compressor (2), a turbine (3), a valve (8), a high-temperature heat exchanger-regenerator (SC-RIG) (5), a condenser/evaporator (6), an ambient pressure tank (1), a high pressure tank (7), a motor/generator (4) and a non-return valve (9).

Component	Assumptions
Heat exchanger-regenerator (SC-RIG) (5)	Pressure loss 1.5% of inlet pressure Exergetic loss
Condenser/Evaporator (6)	Pressure loss 1.5% of inlet pressure
Compressor (2)	Power set at 10000 kW Isentropic efficiency 0.85 Electrical efficiency 0.98 Mechanical efficiency 0.98
Turbine (3)	Isentropic efficiency 0.88 Electrical efficiency 0.98 Mechanical efficiency 0.98
High pressure tank (7)	No temperature and pressure loss
Ambient pressure tank (1)	In balance with atmospheric pressure
Charging time: 4 h	

**Table 1:** Assumptions for each plant component

During the energy storage phase, a compressor with a power set at 10000 kW is employed. See Table 1 for assumptions.

The calculations were made assuming a 4-hour charge duration. Knowing the power of the compressor and the charging time, it is quite easy to obtain the storage capacity.

As presented in the patent by Mr. Spadacini, the ambient pressure tank is a deformable balloon, made of flexible material, preferably plastic (e.g. PVC coated polyester fabric). Alternatively, it may have the structure of a gasometer [6].

Concerning the charging phase, carbon dioxide is in a reservoir in environmental conditions ( $T_A = 293.15$  K;  $P_A = 1.01325$  bar), subsequently the fluid is led through pipes to the compressor inlet (while the turbine outlet is blocked by a valve). The fluid is brought up to a pressure of 65 bar (state C) and to a temperature of 721 K, then it passes through the SC-RIG, storing heat that will be

supplied back during the discharge phase, and it arrives at the condenser inlet (state D).

Then, the fluid passes through the condenser, yielding the heat that will be re-used for the evaporation during the discharge phase. Afterwards, once reached the liquid saturation curve, CO<sub>2</sub> is stored in the tank at a pressure of 63 bar and at a temperature of 297 K (state E).

In Figure 2 the CO<sub>2</sub> charge phase is depicted on the T-s thermodynamic diagram.

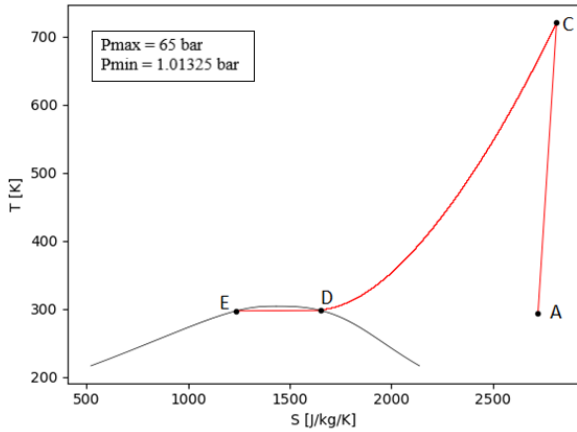


**Figure 2:** CO<sub>2</sub> charge phase on T-s diagram

The discharge phase begins from the high pressure tank. This reservoir has a temperature (297 K) close to the ambient one taken as a reference (293 K), therefore, assuming no pressure losses, the conditions inside the tank could be kept almost constant during the period of time in which the liquid remains there. Thus, the starting point of the discharge phase and the ending point of the charge phase have the same thermodynamic state.

Pressure losses are hypothesized in a similar way to the charge phase for the evaporator and for SC-RIG (see Table 1). Besides, an exergetic loss during the passage through the SC-RIG is considered in order to point out the temperature difference between charge phase (SC-RIG inlet, Fig. 2 state C) and discharge phase (SC-RIG outlet, Fig. 3 state H), due to the SC-RIG thermal effectiveness. The exergetic loss is calculated by reducing the specific enthalpy at the SC-RIG outlet during discharge phase (state H) by 2% compared to SC-RIG inlet during charge phase (state C). The specific enthalpy loss is used to emphasize both a non-perfect adiabaticity of the SC-RIG (minor effect) and its thermal effectiveness < 1 (major effect), i.e. heat is available at a lower temperature during the discharge phase.

During the release phase, the evaporator transfers the previously accumulated heat during condensation, warming the liquid carbon dioxide contained in the tank till it becomes saturated steam (state G). Afterwards, the fluid passes through the SC-RIG absorbing heat until it

reaches the turbine inlet at a temperature of 705 K and a pressure of 61.2 bar (state H). At last, CO<sub>2</sub> expands to generate electrical power and arrives at the ambient pressure tank (state J), which is connected to the turbine outlet by a valve.

In Figure 3 the CO<sub>2</sub> discharge phase is represented on the T-s thermodynamic diagram.

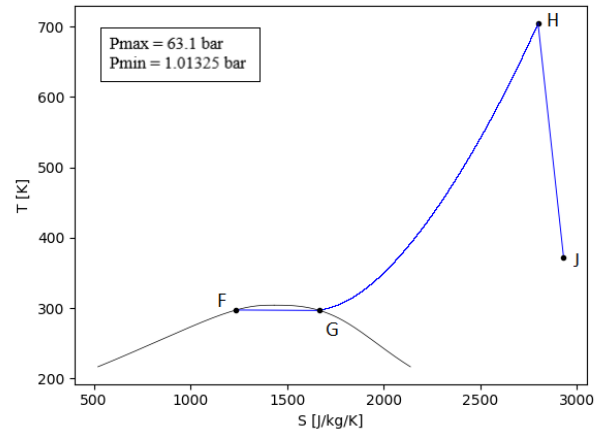


**Figure 3:** CO<sub>2</sub> discharge phase on T-s diagram

### SUPERCRITICAL CO<sub>2</sub> STORAGE SYSTEM

In this paragraph, a CO<sub>2</sub> closed loop in supercritical regime is examined. The system includes: a compressor (2), a turbine (3), a high-temperature (5) and a low-temperature (6) exchanger-regenerator (SC-RIG), an ambient pressure tank (1) and a high pressure tank (7), a motor/generator (4), a valve (8) and a non-return valve (9).

The compressor delivery pressure is assumed 100 bar, as hypothesized in the Spadacini's patent [6].

The characteristics of the compressor (10000 kW), charging time (4 h) and the ambient pressure tank structure are the same as in the previous case. Regarding pressure losses, same prior assumptions are maintained. See Table 2 for assumptions. Two SC-RIGs are used instead of one, because in this way it is possible to compare the heat stored at constant temperature in the subcritical cycle (Fig. 2, line D-E) to the heat stored at low temperature in the supercritical case (Fig. 4, line D-E). The temperature of the CO<sub>2</sub> leaving the high-temperature SC-RIG (5) during the charge phase is set arbitrarily at 373 K (state D), according to the Spadacini's patent [6].

During the accumulation phase, carbon dioxide is in a reservoir in environmental conditions ( $T_A = 293.15$  K;  $P_A = 1.01325$  bar), then the fluid is led through pipes to the compressor inlet (while the turbine outlet is blocked by a valve). The fluid is brought up to a pressure of 100 bar (state C) and to a temperature of 780.6 K (about 60 K higher than subcritical CO<sub>2</sub>), thus going beyond the

critical point. Then, it flows inside the first SC-RIG (C-D line) and next it passes through the second SC-RIG (D-E line). In the end, CO<sub>2</sub> is stored in the high pressure tank at 298.15 K and 97 bar (state E).

Component	Assumptions
High-temperature exchanger-regenerator (high-temperature SC-RIG) (5)	Pressure loss 1.5% of inlet pressure Exergetic loss
Low-temperature exchanger-regenerator (low-temperature SC-RIG) (6)	Pressure loss 1.5% of inlet pressure Exergetic loss
Compressor (2)	Power set at 10000 kW Isentropic efficiency 0.85 Electrical efficiency 0.98 Mechanical efficiency 0.98
Turbine (3)	Isentropic efficiency 0.88 Electrical efficiency 0.98 Mechanical efficiency 0.98
High pressure tank (7)	No temperature and pressure loss
Ambient pressure tank (1)	In balance with atmospheric pressure
Charging time: 4 h	

**Table 2:** Assumptions for each plant component

In Figure 4 the supercritical CO<sub>2</sub> charge phase is depicted on the T-s thermodynamic diagram.

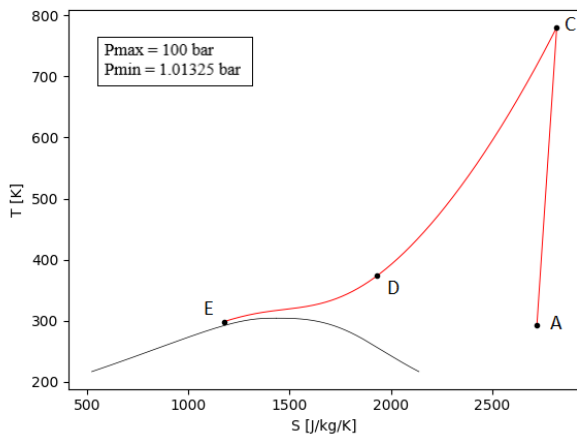


**Figure 4:** S-CO<sub>2</sub> charge phase on T-s diagram

State F, from which the discharge phase begins, is considered equal to state E as assumed in the subcritical case. Pressure losses are hypothesized in a similar way to the charge phase for the two SC-RIGs. In addition, two exergetic losses are considered during the passage through the SC-RIGs. During the release phase, the first SC-RIG heats up the carbon dioxide contained in the tank up to the temperature of 365 K (state G). Afterwards, the fluid passes through the second SC-RIG absorbing heat until it reaches the turbine inlet at a temperature of 763.6 K and a pressure of 94 bar (state H). Finally, CO<sub>2</sub> expands to generate electrical power and arrives at the reservoir at ambient pressure (state J), which is connected to the turbine outlet by a valve. In Figure 5 the supercritical CO<sub>2</sub> discharge phase is represented on the T-s thermodynamic diagram.

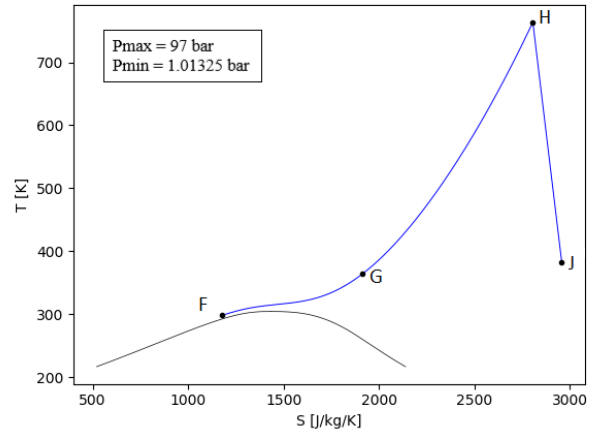


**Figure 5:** S-CO<sub>2</sub> discharge phase on T-s diagram

## RESULTS FOR THE SUBCRITICAL CO<sub>2</sub> CYCLE

For the calculation of the thermodynamic characteristics of fluids, CoolProp 6.4.0 was used, it is an open source library of thermophysical properties, which can be implemented with programming languages such as Python and MATLAB [7].

The assumptions, made for each component, are summarised in Table 1.

Looking at Table 3, a critical aspect encountered is the considerable volume occupied by the reservoir at ambient pressure, which is supposed to be spherical in order to evaluate its diameter. The volume of the ambient pressure tank, before the beginning of the charge phase, contains the working fluid that guarantees a charging time of 4 h and a power of 10000 kW (the CO<sub>2</sub> mass within the tank is equal to 339747 kg). In atmospheric conditions, due to the low density of carbon dioxide (about 1.8 kg/m<sup>3</sup>), large volumes are required to be able to accumulate the entire mass of working fluid. However, despite the high volumes involved, liquified natural gas tanks of such size already exist in the world.

For example, the Adriatic LNG's offshore terminal has a Gravity Based Structure (GBS) which hosts two LNG tanks of 125000 m<sup>3</sup> each [8].

The high pressure tank (supposed spherical as well) must be taken into account. Compared to reservoir at ambient pressure, looking at Table 3, the tank is about seven times smaller in diameter due to the higher accumulated CO<sub>2</sub> density (723 kg/m<sup>3</sup>). When designing the tank, it is of great importance to consider the wide pressure changes that can occur with small temperature variations. Indeed, during the isochoric transformation of liquid CO<sub>2</sub>, reaching 35 °C would mean arriving at a tank pressure of 103 bar. In conclusion, it is necessary for the tank to be adiabatically insulated so that it is not affected by ambient temperature changes, and to be designed by considering stresses significantly higher than the nominal ones.

Since the cycle is subcritical, the CO<sub>2</sub> at high pressure is stored in a liquid phase. As a result, the process is isochoric, but referring to the compressor it is isobar, because as the fluid is gradually compressed, it liquefies in the condenser, in which a free surface of liquefied CO<sub>2</sub> is established (tank is not adiabatic).

Compressor work	423.8 kJ/kg
Heat stored at high temperature	530.3 kJ/kg
Heat stored at constant temperature	124.03 kJ/kg
CO <sub>2</sub> mass flow	23.59 kg/s
Ambient pressure tank diameter	70.66 m
High pressure tank diameter	9.64 m
SC-RIG mass	861.8 t
SC-RIG volume	219.6 m <sup>3</sup>
Turbine work	335.8 kJ/kg
Electrical power in 4 h discharge	7611 kW
RTE	76.1%

**Table 3:** Results for the subcritical CO<sub>2</sub> cycle

As regards the heat exchange, the heat stored at high temperature by SC-RIG (C-D line) is differentiated from that stored at constant temperature (D-E line). It is straightforward to understand that such heat is more relevant than the second both in energy (Tab. 3) and exergetic terms, since in the line D-E the fluid condenses at a temperature of about 297 K. The SC-RIG (component 5 in Fig. 1) has a longitudinal tapered shape in order to ensure a greater heat exchange surface between fluid and constituent material. The SC-RIG is a structured-type regenerator, such as a honeycomb structured, as in [9].

By hypothesis it is chosen a honeycomb constituted by steel, with a vacuum factor of 50%. In the aforementioned article [9] a regenerator made of mullite is analysed; however in this paper the SC-RIG is

assumed consisting of steel, since it is economical, it has good thermo-mechanical characteristics, temperature are intermediate and ceramic materials can be avoided, as they can cause dust release impacting on turbomachinery erosion. Then, a simple calculation was carried out for the preliminary sizing of the SC-RIG. The following steel values are used for the calculations: specific heat capacity  $C_p = 500 \text{ J/kgK}$  and density  $\rho = 7850 \text{ kg/m}^3$ . Figure 6 shows the volumes occupied by the three components taken into account, i.e. the high pressure tank, the reservoir at ambient pressure and the SC-RIG.

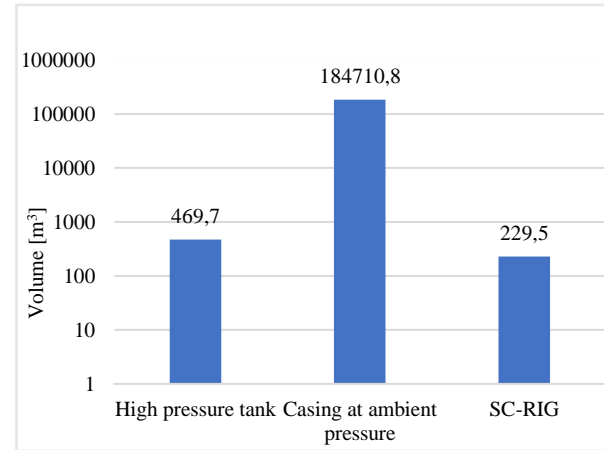


**Figure 6:** Comparison of storage volumes

As indicated in Table 3, the RTE is 76.1%, a value higher or anyway in line with modern advanced CAES solutions [10]. In addition, for a discharge phase that lasts three hours the electrical power generated (10147 kW) is similar to the power required by the compressor; indeed, the drain of the same mass of CO<sub>2</sub> in a shorter time increases the mass flow from 23.6 kg/s to 31.5 kg/s, validating the enhancement of turbine power despite the same specific work.

## RESULTS FOR THE S-CO<sub>2</sub> CYCLE

As regards the results for the supercritical CO<sub>2</sub>, Table 4 shows an increase in the work required by the compressor and in the heat stored at low temperature. The assumptions, made for each component, are summarised in Table 2.

The heat stored increase is due to the higher average temperature at which the heat exchange takes places compared to the subcritical condition; indeed, it is possible to make a comparison between the D-E section with an average temperature value of 297.5 K, for subcritical CO<sub>2</sub>, and the same section for S-CO<sub>2</sub> with a temperature of 336 K.

This analysis, however, may not be entirely correct as the overall heat stored for the subcritical and supercritical charge phase is divided with different

criteria. For S-CO<sub>2</sub>, the temperature of the working fluid coming out of the high-temperature SC-RIG is set at 373 K, while for subcritical CO<sub>2</sub> is equal to 297 K, thus allowing a greater storing of heat. For this reason, the heat stored at high temperature for S-CO<sub>2</sub> is lower than in the subcritical case despite the input temperature of this component is higher.

Compressor work	490.13 kJ/kg
Heat stored at high temperature	486.37 kJ/kg
Heat stored at low temperature	248.2 kJ/kg
CO <sub>2</sub> mass flow	20.4 kg/s
Ambient pressure tank diameter	67.3 m
High pressure tank diameter	8.84 m
High-temperature SC-RIG mass	598.5 t
High-temperature SC-RIG volume	152.5 m <sup>3</sup>
Turbine work	391.1 kJ/kg
Electrical power in 4 h discharge	7664 kW
RTE	76.6%

**Table 4:** Results for supercritical CO<sub>2</sub>

A positive aspect found for S-CO<sub>2</sub> is the reduction of the occupied volumes, which involves a slight decrease in plant size and construction costs.

Since the specific work of the turbine and compressor increases compared to the subcritical case, while the power of the latter remains unchanged, the mass flow of working fluid decreases and consequently, for a charging time of 4 hours, a lower CO<sub>2</sub> mass will be required (294 ton versus 340 ton). In addition, the slight lowering of the diameter of the high pressure tank is also linked to an increase in CO<sub>2</sub> density inside it (812.7 kg/m<sup>3</sup> versus 723 kg/m<sup>3</sup>).

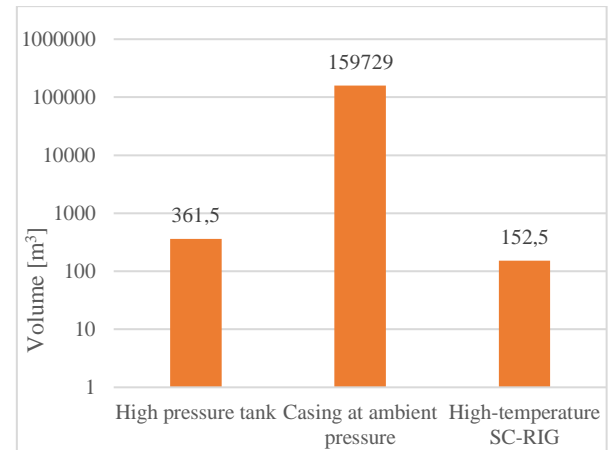
Moreover, the high pressure tank is isochoric, which means that the overall process is transient by definition. To ensure a quasi isobaric pressure for the compressor/turbine during operation, it is possible to employ variable volume storage (e.g. with mobile internal membrane) or to exploit a thermal regulation (i.e. at the beginning of the charge phase it is possible to keep a higher storage temperature, and toward the end of the charge phase the temperature is lowered, increasing the density of CO<sub>2</sub>). In addition, in supercritical regime, the density of the fluid varies greatly with temperature, therefore the storage temperature can be modulated in order to keep the pressure constant. So, referring to the high pressure tank, if the volume is constant, pressure may be kept also constant by a not adiabatic transformation.

In Table 4, SC-RIG volume is less than the subcritical case, because it has a lower heat exchanged and a higher temperature difference.

The low-temperature SC-RIG, on the other hand, is not analysed in detail, but problems related to a considerable heat storage, with a limited temperature difference of the component, can be supposed.

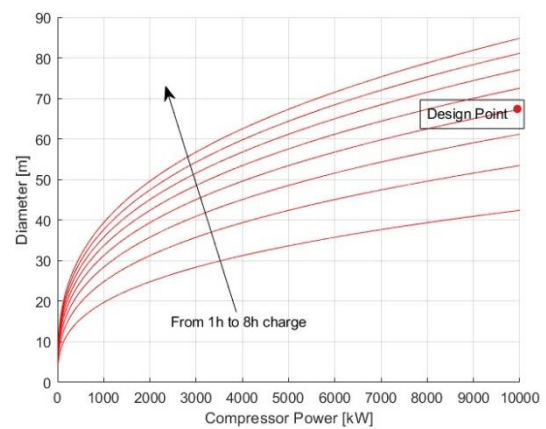
At last round trip efficiency (RTE) gains a slight percent increase going supercritical.

Figure 7 shows the volumes occupied by the three components taken into account, i.e. the high pressure tank, the reservoir at ambient pressure and the high-temperature SC-RIG.



**Figure 7 :** Comparison of storage volumes for S-CO<sub>2</sub>

However, it is possible to reduce the volume of the ambient pressure tank by acting on the charging times or power of the system in order to decrease the mass of CO<sub>2</sub> inside, but at the expense of the amount of energy that can be stored and the efficiency of the system. Figure 8 shows the trend of the ambient pressure tank volume as the charging time and power of the compressor change.



**Figure 8:** Ambient pressure tank diameter as a function of power and charging time

### COMPARATIVE ANALYSIS

In the following paragraph a comparative analysis is carried out between some results obtained from different types of working fluid. Furthermore, Adiabatic Compressed Air Energy Storage (ACAES) is included as benchmark, since it works in a similar way to the cycles seen above.

In addition to carbon dioxide, other working fluids such as N<sub>2</sub>O, SF<sub>6</sub> and H<sub>2</sub>O are considered. The main assumptions used for CO<sub>2</sub> remain valid for other substances (see Tables 1 and 2). As regards the water, to maintain a similarity with the systems analysed previously, the minimum pressure is set to 0.05 bar and maximum pressure to the atmospheric one.

The first parameter considered is round trip efficiency (RTE), which is one of the main features of energy storage systems.

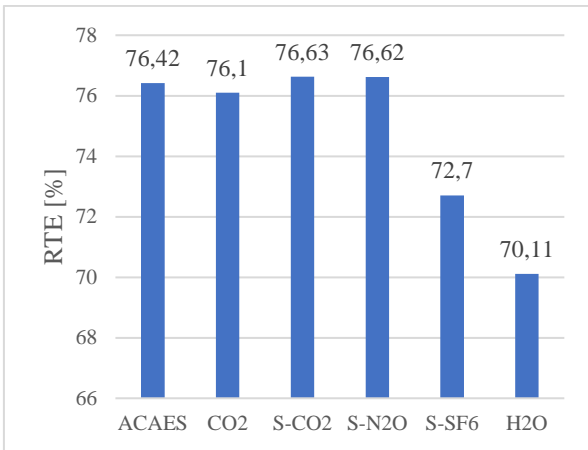


**Figure 9:** Comparison of RTE values

The second parameter taken into account is the volume of the reservoir (at a pressure of 0.05 bar for H<sub>2</sub>O and at ambient pressure for other fluids). Then, this comparison allows to identify the fluid that, during the design phase, guarantees the smallest footprint of the accumulation volume.

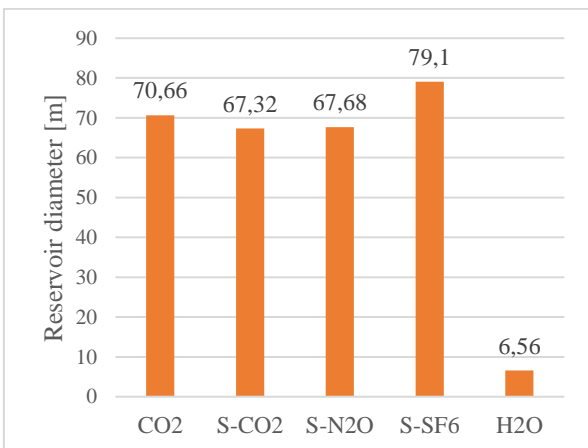


**Figure 10:** Comparison of reservoir diameters

Water is considered as a working fluid because the space required for accumulation will be reduced, thanks to the fact that at environmental conditions it can be easily stored in the liquid phase and therefore at a higher density than gases.

Comparison of masses of the various heat exchangers-regenerators (SC-RIG) is illustrated in Figure 11.

In addition, considering an average steel price of 0.90 €/kg, for configuration with CO<sub>2</sub> as a working fluid it would cost about € 800000, which clearly indicates its potential impact on system capital cost.

For S-SF<sub>6</sub> the value is high due to the increased mass flow rate in circulation and the lower ΔT of the SC-RIG.

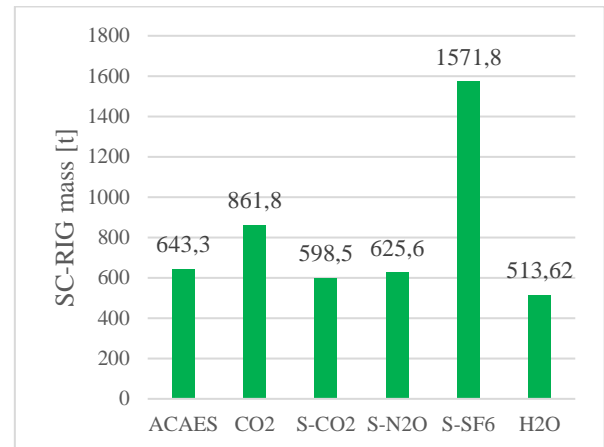


**Figure 11:** Comparison among SC-RIG weights

Finally, the ratio between the specific work of the compressor and the total stored heat is introduced as a comparison factor. For CO<sub>2</sub> and H<sub>2</sub>O, the total heat is obtained from the sum between the one stored at high temperature (inside the SC-RIG) and the heat absorbed at a constant temperature during the phase change.

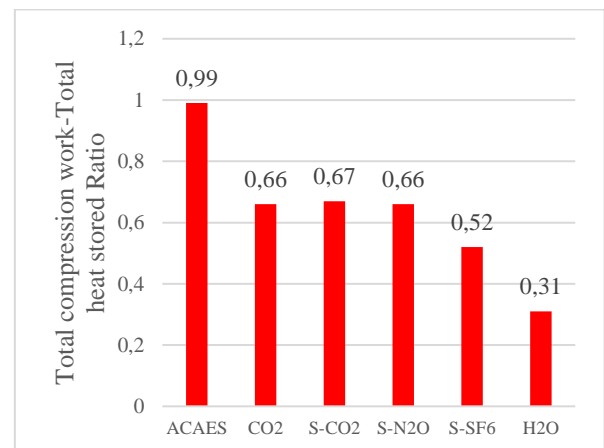


**Figure 12:** Comparison of compression work to stored heat ratios

For S-CO<sub>2</sub>, S-N<sub>2</sub>O and S-SF<sub>6</sub> the total heat is obtained from the sum between the heat stored at high

temperature (inside the high-T SC-RIG) and the heat absorbed at low temperature (inside the low-T SC-RIG). Water has a low value of this ratio (0.31) due to the high latent heat.

The analysis shows that the fluid able to guarantee the best performance, referring to RTE, is CO<sub>2</sub> in supercritical conditions. Furthermore, S-CO<sub>2</sub> is also competitive in the comparison among SC-RIG weights (Fig. 11) and in the comparison of reservoir diameters (Fig. 10), neglecting H<sub>2</sub>O.

Anyway, since the performance of CO<sub>2</sub> and S-CO<sub>2</sub> is quite similar, it may not be worth complicating the plant using higher pressures. Therefore, it could be better opting for the subcritical cycle that would allow an easier management of high pressure tank despite a small decrease RTE.

Table 5 compares the parameters of greatest interest for the working fluids considered most suitable.

Working fluid	CO <sub>2</sub>	S-CO <sub>2</sub>	H <sub>2</sub> O
RTE [%]	76.1	76.6	70.1
Electrical power [kW]	7611	7664	7012
Compression work [kJ/kg]	423.84	490.13	975.54
Heat stored at high-T [kJ/kg]	530.28	486.37	837.45
Reservoir diameter [m]	70.66	67.32	6.56
Tank diameter [m]	9.64	8.84	6.65

**Table 5:** Comparison between the most relevant parameters

## CONCLUSIONS

The paper provides an overview of innovative energy storage systems via closed-loop cycles, assessed through a detailed but relatively straightforward thermodynamic analysis of the cycle.

Among the different working fluids considered (CO<sub>2</sub>, N<sub>2</sub>O, SF<sub>6</sub> and H<sub>2</sub>O), the substance that guarantees the best performance, referring to RTE, is CO<sub>2</sub> in supercritical conditions (RTE = 76.6%).

Furthermore, an investigation was conducted for each fluid concerning the size of the tanks at atmospheric pressure, assumed spherical. It was found that for CO<sub>2</sub>, N<sub>2</sub>O and SF<sub>6</sub> the diameter of these components is a critical aspect to be carefully considered (for S-CO<sub>2</sub> the diameter is 67.32 m).

This system may seem similar to ACAES, with the advantage of constant pressure ratio, thanks to the CO<sub>2</sub> change of state (or cooling, in case of supercritical cycle).

In the future, it will be essential to carry out a comprehensive techno-economic analysis of the SC-RIG and the heat exchangers, since they are fundamental

components for the operation of the entire plant and they contribute to the overall efficiency and cost. Moreover, it will also be essential to study the dynamic behaviour of this storage system, using analogies and results from other application of CO<sub>2</sub> in power systems (e.g. [11]), in order to better understand the possible applications of this technology in the energy market.

## NOMENCLATURE

CSP	Concentrated Solar Power
RTE	Round Trip Efficiency
SC-RIG	Heat Exchanger-Regenerator
S-CO <sub>2</sub>	CO <sub>2</sub> in supercritical condition
S-N <sub>2</sub> O	N <sub>2</sub> O in supercritical condition
S-SF <sub>6</sub>	SF <sub>6</sub> in supercritical condition
WHR	Waste Heat Recovery

## REFERENCES

- [1] IEA (2020). World Energy Outlook 2020. France, Paris.
- [2] IEA (2020). Global Energy Review 2020. France, Paris.
- [3] Oudalov, A.; Chartouni, D.; Ohler, C.; Linhofer, G. (2006). Value Analysis of Battery Energy Storage Applications in Power Systems. Power Systems Conference and Exposition. PSCE '06. 2006 IEEE PES, pp.2206-2211.
- [4] Karmiris G.; Tengnér T. (2013). Peak Shaving Control Method for Energy Storage. Sweden, ABB AB, Corporate Research Center, Västerås.
- [5] Marchionni, M.; Bianchi, G.; Tassou, S. (2020). Review of Supercritical Carbon Dioxide (sCO<sub>2</sub>) Technologies for High-grade Waste Heat to Power Conversion. SN Applied Sciences 2(4), DOI: 10.1007/s42452-020-2116-6.
- [6] Spadacini, C.; Inventor (2020). Energy Storage Plant and Process. Italy, Milan. Patent WO 2020/039416 A2.
- [7] Bell, I. H.; Wronski, J.; Quoilin, S.; Lemort, V. (2014). Pure and Pseudo-pure Fluid Thermophysical

- Property Evaluation and the Open-Source Thermophysical Property Library CoolProp. *Industrial & Engineering Chemistry Research* 2014 53 (6), 2498-2508. DOI: 10.1021/ie4033999
- [8] RINA Consulting S.p.A.; Adriatic LNG (2019). Documentazione Tecnica Allegata alla Domanda di Riesame dell'AIA, Sintesi non Tecnica. Italy, Genoa.
- [9] Mahmood, M.; Traverso, A.; Traverso, A. N.; Massardo, A. F.; Marsano, D.; Cravero, C. (2018). Thermal Energy Storage for CSP Hybrid Gas Turbine Systems: Dynamic Modelling and Experimental Validation. *Applied Energy* 212 (2018) 1240–1251. Italy, Genoa.
- [10] Wang, J.; Lu, K.; Ma, L.; Wang, J.; Dooner, M.; Miao, S.; Li, J.; Wang, D. (2017). Overview of Compressed Air Energy Storage and Technology Development. *Energies* 2017 10 (7), 991. Switzerland, Basel.
- [11] Lambruschini, F.; Liese, E.; Zitney, S.E.; Traverso, A. (2016). Dynamic Model of a 10 MW Supercritical CO<sub>2</sub> Recompression Brayton Cycle. ASME Paper GT2016-56459, BEST PAPER AWARD.

# DuEPublico

Duisburg-Essen Publications online

UNIVERSITÄT  
D U I S B U R G  
E S S E N

*Offen im Denken*

ub | universitäts  
bibliothek

*Published in: 4th European sCO2 Conference for Energy Systems, 2021*

This text is made available via DuEPublico, the institutional repository of the University of Duisburg-Essen. This version may eventually differ from another version distributed by a commercial publisher.

**DOI:** 10.17185/duepublico/73956  
**URN:** urn:nbn:de:hbz:464-20210330-102746-9



This work may be used under a Creative Commons Attribution 4.0 License (CC BY 4.0).